Geochemistry, Geophysics, Geosystems

RESEARCH ARTICLE
10.1029/2019GC008276

Constraints on Fe-Oxide Formation in Monsoonal Vertisols of Pliocene Kenya Using Rock Magnetism and Spectroscopy

Christopher J. Lepre[1,2]

[1]Department of Earth and Planetary Sciences, Rutgers University, Piscataway, NJ, USA, [2]Lamont-Doherty Earth Observatory, Columbia University, Palisades, NY, USA

Key Points:
- Monsoonal Vertisols of Pliocene Kenya have deep dry season water tables and are strongly magnetic relative to Vertisols at higher latitudes
- Bimodal rainfall seasonality and the frequency of moisture extremes cause the redox conditions to produce high magnetite concentrations
- Mean annual rainfall during pedogenesis is estimated as <200 mm and between 500-1000 mm, agreeable with other Pliocene records for the area

Correspondence to:
C. J. Lepre,
clepre@eps.rutgers.edu

Citation:
Lepre, C. J. (2019). Constraints on Fe-oxide formation in monsoonal Vertisols of Pliocene Kenya using rock magnetism and spectroscopy. *Geochemistry, Geophysics, Geosystems*, *20*. https://doi.org/10.1029/2019GC008276

Received 18 FEB 2019
Accepted 13 AUG 2019
Accepted article online 14 OCT 2019

Abstract Pliocene Vertisols from the Turkana Basin of northwest Kenya (~4°N latitude) have been examined using isothermal remanent magnetization (IRM) experiments, susceptibility measurements, and diffuse reflectance spectroscopy. The complete vertical profile of each paleosol is almost intact, measuring >2 m in thickness and being strongly magnetic (IRM at 1.0T ranges from 4 to 25 $\times 10^{-3}$ Am^2/kg). Downprofile changes to the proxy indicators suggest uninterrupted pedodevelopment and a lack of stratigraphic inversions caused by argilli-pedoturbation. Magnetic minerals consist of hematite to a lesser degree, and pedogenic ferrimagnets derived from moisture cycles that were controlled by monsoonal rainfall. Basal pedogenic zones of the paleosols are magnetically intense, and preserve the greatest slickenside development indicating pronounced seasonal wetting and drying. These observations indicate a deeper dry season water table as compared to poorly drained temperate/tropical Vertisols, which suffer reductive dissolution of Fe oxides in basal pedogenic horizons associated with weak magnetic intensities. Magnetic susceptibilities and the well-represented presence of fine pedogenic ferrimagnets suggest that Pliocene rainfall was greater than the local modern rate of 200 mm/year and may have been within the range of 500–1,000 mm/year. The study highlights the need to expand the database on Vertisols Fe oxides and magnetism, especially considering the anomalously dry and bimodal rainfall seasonality of East Africa.

1. Introduction

Vertisol is a major soil order important for ecological management and agricultural practices worldwide (Ahmad, 1983; Chittamart et al., 2010; Jean Pierre et al., 2019; Nordt et al., 2004; Wilding & Puentes, 1988; Yaalon & Kalmar, 1978). Vertisols are used frequently for paleoenvironmental reconstructions since they are found in all eras of the Phanerozoic (Beverly et al., 2018; Nordt & Driese, 2010; Retallack, 1988). Despite being well studied through time, across geography, and in application, there is paucity of research on the magnetic-mineral properties of Vertisols, especially in geologic settings (Jordanova, 2017).

Along with expandable clays as the substrate, seasonal saturation with moisture followed by desiccation is the control on Vertisol pedogenesis (Ahmad, 1983; Wilding & Puentes, 1988; Yaalon & Kalmar, 1978). Vertisols cannot form without these ingredients. East Africa is an opportune setting for Vertisol pedogenesis because of the monsoonal delivery of seasonal rainfall and ample volcanic terranes available for smectite clays (Deckers et al., 2001). Geological studies on East African Vertisols historically have focused on the stable isotopic composition of carbonate nodules (Cerling et al., 2011; Levin et al., 2011; Quinn & Lepre, 2019; Wynn, 2004, 2000). Yet new work is emerging on bulk paleosol geochemistry (Beverly et al., 2018). Most of this research is conducted at hominin fossil and archaeological sites for the purpose of understanding how paleomonsoonal climates influenced the evolution of humans. Besides magnetostratigraphy for age control (e.g., Hillhouse et al., 1986; Lepre & Kent, 2015), none of the research provides data on paleosol magnetism/magnetic minerals related to paleoenvironmental conditions.

In this study, Pliocene Vertisols of the Koobi Fora formation exposed on the east side of Lake Turkana in northwest Kenya are examined for properties related to their magnetic mineral contents. Brown and Feibel (1986) have documented the stratigraphic distribution of the Vertisols within the Koobi Fora formation. Lepre (2017) studied the occurrence of Vertisols associated with fluvial avulsion deposits from

Pleistocene intervals of the formation. Johnson and Raynolds (1976) were among the first to recognize the presence of vertic features and relate these to past environmental conditions for the formation. More extensive taxonomic, morphologic, and geochemical study of Pliocene Vertisols has been conducted on the west side of the Turkana Basin (Wynn, 2000). Further examination of the Pliocene Vertisols, especially their magnetic minerals and related properties, is warranted because of the need to refine the context of the rich record of human evolution from Turkana (Brown et al., 2013; Leakey et al., 1998).

Fe oxides (oxides, hydroxides, and oxyhydroxides) of soils are particularly conducive for reconstructing past environments, as these minerals tend to be abundant at Earth's surface and are sensitive indicators of redox conditions and moisture (Bigham et al., 2002; Wu et al., 2019). Extensive analyses of soil magnetism have resulted from work with loess sequences (Geiss et al., 2008; Maher et al., 2003), especially those from China (Kukla et al., 1988). This work has demonstrated that many modern and fossil soils have upper horizons enhanced with magnetic minerals as a consequence of moisture, redox, and/or temperature conditions (Ahmed & Maher, 2018). However, it is not well understood how enhancement processes develop and interact over the seasonal cycle of a soil and throughout the maturation history of a vertical soil profile. Furthermore, the style of soil magnetic enhancement varies according to regional setting. In monsoonal soils from the Chinese loess plateau, for example, magnetic enhancement often is measured through contrasts in stable single domain and superparamagnetic fractions (Maher, 2016; Maher & Thompson, 1995). Other settings, like dry Mediterranean soils, the magnetic enhancement proceeds through different suites of magnetic minerals exhibiting a narrower grain size distribution (Torrent et al., 2010, 1980). Vertisols also show magnetic enhancement in upper horizons, although this is based upon observations from only three detailed studies (Fischer et al., 2008; Jordanova & Jordanova, 2016; Lindquist et al., 2011). Enhancement of upper horizons of Vertisols may proceed passively, as a result of shallow depths for the dry season water table causing reductive dissolution of Fe oxides from lower Vertisol horizons (Fischer et al., 2008), or actively through seasonal wetting (anaerobic) and drying (aerobic) events that facilitate the formation of Fe^{2+}/Fe^{3+} needed to produce ferrimagnetic particles (Taylor et al., 1987). Considering the paucity of observations, the Pliocene soils from the Turkana Bain of Kenya provide an ideal opportunity to further constrain factors contributing to Vertisol magnetic mineral properties. Because of the East African climate, these Pliocene Vertisols may demonstrate similarities with the monsoonal soils of the Chinese loess plateau that show strong magnetic enhancement from nanoscale pedogenic Fe oxides. To test these ideas, two Pliocene Vertisols from Turkana are examined for mineral constituents. A nearly complete vertical profile for each paleosol was studied with a combination of rock magnetism and diffuse reflectance spectroscopy. Results differ from published Vertisol examples and add to this emerging research on Fe oxides and magnetism. These new observations highlight the anomalous dryness and bimodal rainfall seasonality of the East African equatorial monsoon and the need to understand the depth of seasonal water table variations in order to explain the magnetic and mineral distributions of the soil profile.

2. Materials and Methods

2.1. Paleosol Samples

Fossil collection Area 207 is located on the northeast side of Lake Turkana in Kenya (Figure 1a). Pliocene paleosols in Area 207 are exposed along the valley walls and banks of ephemeral streams, and most are located at well-drained, stable upland positions. Sedimentary outcrops dominate the geologic exposures and consist of continental siliciclastic detritus with paleosols overprinted on mudstones. The local chronostratigraphy is well documented and based upon magnetostratigraphy and tephrochronology (Figure 1b). Lithological descriptions of the outcrops and the lithostratigraphic nomenclature of Area 207 are reported in Brown and Feibel (1986). These authors describe the stratigraphic distributions of multiple paleo-Vertisols based on the presence of ancient mukkara structures, gilgai topography, and pseudo anticlines. Paleogeographic reconstructions for the Pliocene Turkana Basin suggest that the paleo-Vertisols formed within low-lying areas of alluvial plains and flood basins (Bruhn et al., 2011).

The focus of this work was on two paleo-Vertisols (i.e., 207TB-7 and 207TB-9) with nearly complete vertical profiles. Paleosol 207TB-9 is constrained by the reverse subchron C2An.2r (Mammoth subchron) dated between 3.33 and 3.22 Ma, and 207TB-7 is constrained by normal subchron C2An.2n dated at 3.22–3.11 Ma (Figure 1b). They thus formed at different periods and probably are separated by an interval of time

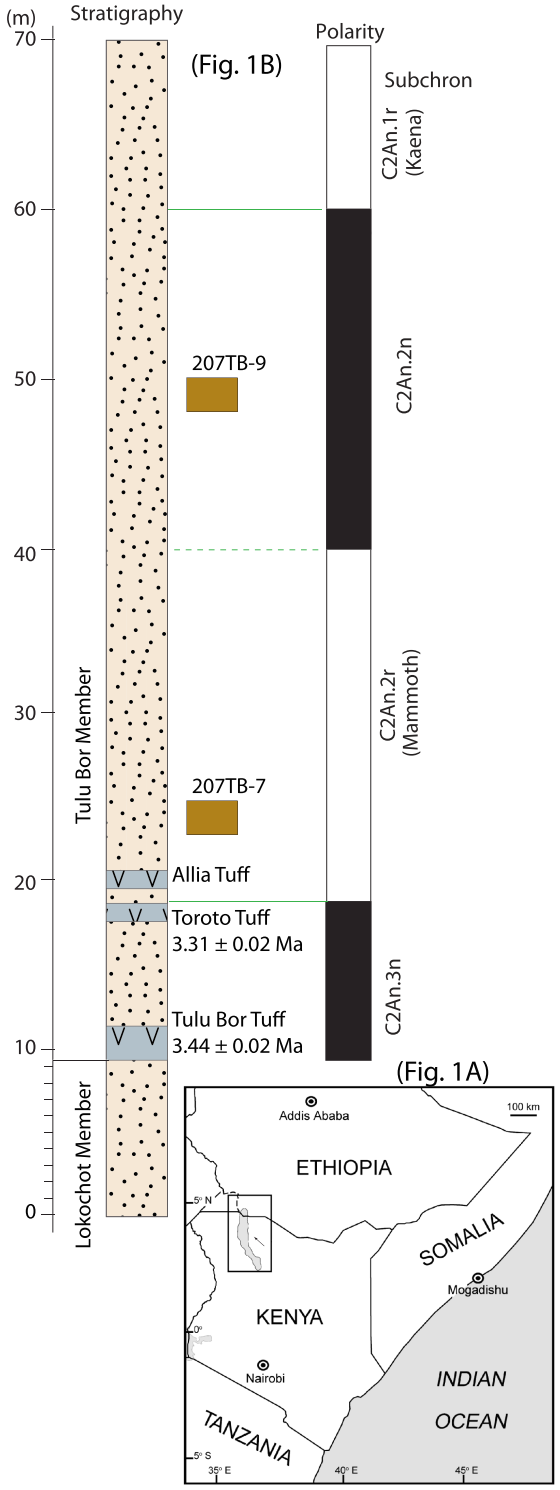

Figure 1. Geographic and stratigraphic context of the study. (a) The location of the Lake Turkana basin within Kenya and Ethiopia. Boxed area of the map is the approximate extent of the basin with the arrow pointing to fossil collection Area 207. (b, left to right) The position of the paleosols within the local stratigraphy of Area 207 (Brown & Feibel, 1986) along with ash beds correlated to radiometrically dated horizons (McDougall et al., 2012), and the magnetostratigraphy of Area 207 (Hillhouse et al., 1986). Geomagnetic Polarity Time Scale of Cande and Kent (1995).

lasting on the order of 10^3–10^4 years. In order to understand how magnetic properties and Fe oxides vary, the two paleosols were systematically sampled downprofile from surface horizon to parent material. From each level, irregularly shaped hand-cut blocks measuring ≥30 cm^3 were collected after narrow trenches (~0.5 m deep) were excavated into the outcrops. Each data point in Figure 2 represents an observation made on a subsample of a block, which were taken at 10, 50, 100, 150, and 200 cm relative to the topmost part of the paleosol.

2.2. Diffuse Reflectance Spectroscopy

Diffuse reflectance spectroscopy (DRS) is used to interpret the types of magnetic minerals and their concentrations within the paleosols (Deaton & Balsam, 1991; Hu et al., 2016; Scheinost et al., 1998). This method determines sample composition through quantifying the interaction between visible light and the properties imparted to a soil/paleosol by Fe oxides. For this study, two DRS analyses were applied to identifying hematite content of the Area 207 paleosols: (1) sample redness and (2) the second derivative of reflectance. Redness was determined from the percentage reflectance of a sample within the VIS range, normalized by the reflectance of a white standard. The normalized percentage reflectance values within the wavelength band for red, 630–700 nm, then were summed and the average calculated (Long et al., 2011).

The second derivative of the VIS reflectance is used to assess the hematite concentrations of the samples. Scheinost et al. (1998) demonstrated that the second derivative curve of the Kubelka-Munk remission function of reflectance quantifies the hematite concentrations of natural and lab-prepared samples. These authors identified hematite through the second-derivative amplitude between the ~535-nm minimum and the ~580-nm maximum. The height of the second derivative peak, that is, the intensity of the wavelength, increases with hematite concentration and the position of the minimum and maximum occurs at different wavelengths as hematite concentration changes and ion substitutions for iron increase (Deaton & Balsam, 1991; Hu et al., 2016; Liu et al., 2011).

DRS measurements were made using a Varian Cary 50 photospectrometer fitted with an external integrating sphere. Precision and accuracy of the machine has been determined with a series of mixed hematite and calcium carbonate powders in concentrations ranging from 0.01 to 20.0%. Calibration experiments using a particular concentration standard is repeatable to <5% of the measured amplitude intensity. Error for wavelength determinations is less than 0.1%. The photospectrometer is capable of differentiating hematite concentrations of 0.1–4.0% in a calcium carbonate (approximately white) matrix. Detailed DRS experiments suggest the lower limit of hematite detection in standardized samples with a dark-colored, reflectance-attenuating matrix is a concentration of 0.05% (Balsam et al., 2014).

2.3. Rock Magnetic Experiments

Paleosols samples were reduced into orthogonal specimen cubes with a volume of ~10 cm^3, weighed, and scribed with inventory numbers and fiducial marks using nonmagnetic, heat resistant ink. All magnetic remanence measurements for the specimens were determined with a 2G Model 760 DC- SQUID rock magnetometer housed in the shielded room of the Paleomagnetics Laboratory of Lamont-Doherty Earth Observatory

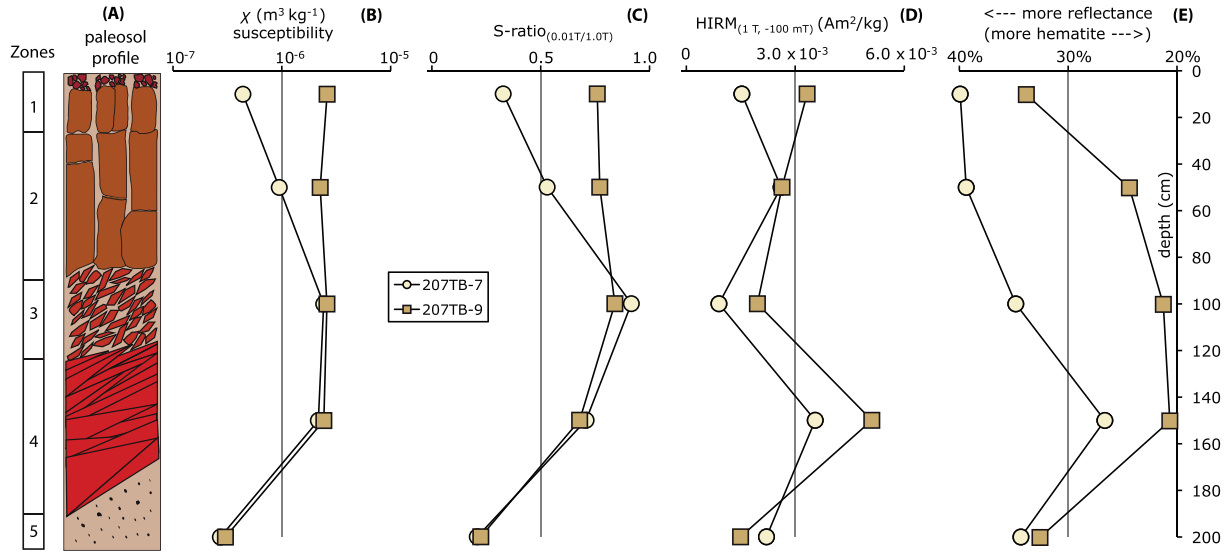

Figure 2. Morphology, magnetism, and spectroscopy of Paleo-Vertisols 207TB-7, 207TB-9. (a) Downprofile changes in Vertisol structure and zonation scheme of Dudal and Eswaran (1988), (b) variations of mass specific susceptibility, (c) S-ratio with applied fields indicated in T, (d) HIRM with applied fields indicated in T, and (e) % VIS light reflectance within the red range (630–700 nm) normalized to a white standard. For both paleosols a sample was collected at 10, 50 100, 150, and 200 cm. The zero datum was the topmost stratigraphic level of zone 1. Each circle or square represents a measurement for a single sample.

(Columbia University, NY, USA). Bulk magnetic mineralogy of the specimens was constrained through magnetic susceptibility and a series of isothermal remanent magnetization (IRM) experiments described below. Magnetic susceptibility was determined with a Bartington MS2B instrument. IRM treatments were applied with an ASC impulse magnetizer using a 1.25″ coil.

Following the method of (Lowrie, 1990), the thermal demagnetization (TD) of orthogonal IRM fields applied to a specimen was used to identify ferromagnetic minerals based on coercivity and unblocking temperature properties. This involved applying a 2,500-mT IRM along the $+z$ axis of a specimen and a 150-mT field along the $+y$ axis. Specimens then were treated to progressive heating steps at 100, 200, 300, 400, 500, 600, 625, 650, and 675 °C using an ASC thermal demagnetizer.

The HIRM, that is, "hard" IRM, is a method used to study the high-coercivity minerals hematite and goethite (Bloemendal et al., 1992; Liu et al., 2007; Thompson & Oldfield, 1986). The approach of Hu et al. (2016) defines the HIRM as

$$\mathrm{HIRM}\left(_{\mathrm{FF,BF}}\right) = (\mathrm{IRM_{FF}} + \mathrm{IRM_{BF}})\div;2$$

In this analysis, $\mathrm{IRM_{BF}}$ is a back-field IRM that is smaller than the forward-field IRM, abbreviated $\mathrm{IRM_{FF}}$. Paleosols specimens treated to HIRM study were first given an $\mathrm{IRM_{FF}}$ imparted along the $+z$ axis and then a $\mathrm{IRM_{BF}}$ along the $-z$ axis using fields of 1,000 and 100 mT respectively. The S-ratio is another approach for interpreting the relative magnetic abundance preserved within rock, sediment, and soil samples (Bloemendal et al., 1992). A ratio closer to one (zero) indicates a predominance of low- (high-) coercivity minerals such as magnetite and maghemite (hematite and goethite). In this study, the S-ratio is defined as $\mathrm{IRM_{BF}}/\mathrm{IRM_{FF}}$.

Select specimens were treated to back-field IRM experiments. This involved exposing the specimen to a single IRM treatment at 2,500 mT acquired along the $-z$ axis, followed by a series of progressively higher IRM fields along the $+z$ axis using the following steps: 20, 40, 60, 80, 100, 150, 200, 250, 300, 500, 750, 1,000, 1,250, 1,500, 1,750, 2,000, 2,250, and 2,500 mT.

3. Results

3.1. Vertisol Horizons

Horizonation for paleo-Vertisols 207TB-7 and 207TB-9 (Figure 2a) share characteristics with the five-zone model described by Dudal and Eswaran (1988). Comparison to the model suggests that the Area 207

paleosols are similar to a Typic Chromustert or Paleustollic Chromustert. Diagnostic features of zone 1 (uppermost horizon) to 5 (parent material) for the Area 207 paleosols are

1. Angular/blocky structures and some prismatic peds up to 20 cm high, but structures commonly 1–5 cm
2. Prisms up to 50 cm high, but commonly 10–20 cm; first slickensides appear
3. Wedge-shaped slickensided structures
4. Larger wedge-shaped slickensided structures and synclinal forms
5. Massive mudstone with a few slickensides

Wynn (2000) has recognized similar Pliocene paleo-Vertisols at outcrops southwest of Lake Turkana. He names these as the "Aberegaiya pedotype" and interprets the Aberegaiya as Typic Calciusterts (USDA classification) or Chromic Vertisols (FAO classification). Paleo-Vertisols from Area 207 preserve sparse amounts of carbonate nodules the size of small pebbles to granules, a featured shared with other Pliocene soils of the basin (Levin et al., 2011; Quinn & Lepre, 2019; Wynn, 2004, 2000). Pedogenic carbonate nodules usually indicate a net deficit of effective moisture associated with the dry seasons of the East African monsoon (Cerling, 1984).

3.2. Proxy Indicators of Fe Oxides

Overall, the proxy indicators for the two paleosols lack erratic shifts in the downprofile changes to the magnetic Fe oxides (Figure 2). Upper horizons of 207TB-7 have comparatively low values for the proxy indicators; however, the values smoothly increase downprofile as part of a systematic increase to higher concentrations in zones 3 and 4. These downprofile changes suggest uninterrupted pedogenesis without evidence of multiple generations of soils overlapping their development through the same substrate (Geiss et al., 2008; Lindquist et al., 2011). Each paleosol is interpreted to represent a single phase of soil development without significant reworking of the substrate by Vertisols processes, which may cause irregular downprofile changes to magnetic and DRS data, resulting in a more ambiguous signal. The data do not provide evidence of strong mixing by pedoturbation, adding to a growing consensus that the "inversion" model does not adequately explain all Vertisol formation (Driese et al., 2013; Nordt et al., 2004). However, it should be noted that mixing and stratigraphic inversions may occur near the margins of gilgai topography and synclines (Kovda et al., 2001).

Mass specific susceptibility values span the same 2 orders of magnitude for 207TB-7 and 207TB-9 (Figure 2b). Parent material (i.e., zone 5) for each paleosol registered the lowest values. By a factor of almost 5, susceptibility for 207TB-7 increases downprofile from zone 1 to zones 3 and 4. The largest susceptibility for 207TB-9 was from zones 3 and 1; however, there is not significant variation to the values for zones 1–4 (Figure 2b).

In both paleosols, the largest S-ratio is for zone 3 and the smallest is for zone 5 (Figure 2c). The S-ratios are similar for zone 3 (0.84, 207TB-9; 0.92, 207TB-7), zone 4 (0.68, 207TB-9; 0.71, 207TB-7), and zone 5 (0.21, 207TB-7; 0.23, 207TB-9). S-ratios for 207TB-7 increase from zone 1 (0.33) to zone 2 (0.53) before reaching the maximum in zone 3. S-ratios for 207TB-9 vary little through zones 1–4 (0.76–0.84).

HIRM data (Figure 2d) suggest that zone 4 of 207TB-9, followed by zone 4 of 207TB-7, has the largest concentration of magnetically hard minerals. The HIRM of paleosol 207TB-9 decreases linearly through zones 1–3 before increasing in zone 4 and then decreasing in zone 5. The HIRM profile curve of 207TB-7 displays a somewhat similar pattern, except there is an increase in zone 2. The DRS (Figures 2e and 3) and HIRM (Figure 2d) data suggest that the highest concentration of hematite occurs within zone 4 of both paleosols. However, the HIRM generally decreases through zones 1–3 while the DRS suggests hematite concentration increases through these zones. The data resolved by the two proxy indicators need not agree entirely because the HIRM is dependent on the magnetization of hematite, whereas the DRS data are dependent upon grain surface area, which is related to grain size. Small magnetic particles (e.g., superparamagnetic grains) are incapable of carrying a remanence from IRM (Harrison & Feinberg, 2009) yet still detectable through DRS as red soil color is derived from and enhanced by the abundance of very fine hematite grains (Torrent & Barrón, 2003).

TD of orthogonal IRM fields (Figures 4a–4d) suggests that the parent material (zone 5) and upper horizons (e.g., zone 3) contain a similar assemblage of magnetic mineral types consisting of hematite and maghemite/magnetite. Yet the IRM values indicate a substantial increase of the ferrimagnetic phases in zone 3 as compared to zone 5 for example. No appreciable decreases in the high-coercivity component is

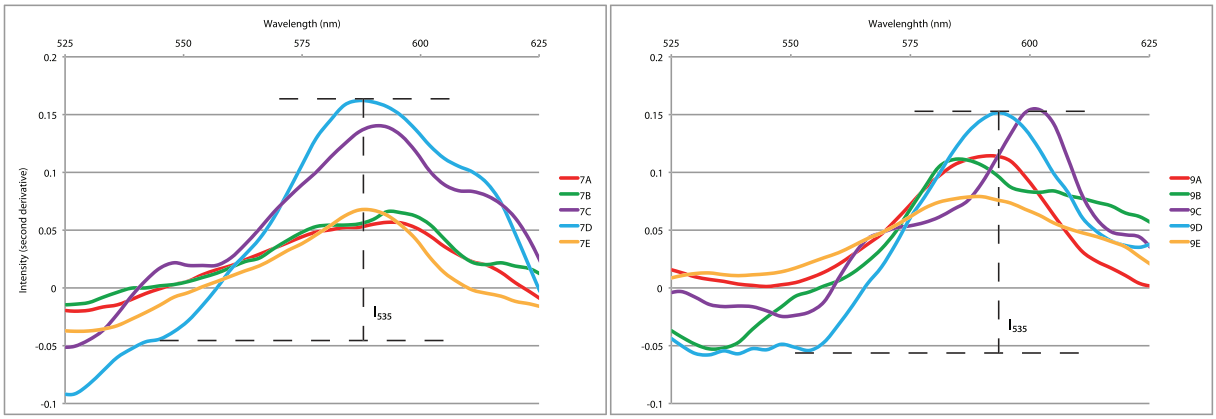

Figure 3. DRS data of individual sample levels. (left) Second derivative of the K-M remission function for paleosol 207TB-7. Vertical scale is intensity and horizontal scale is nanometers. The wavelength interval is restricted to the characteristic band position for determining hematite concentration between about 535 and 580 nm as recommended by Scheinost et al. (1998). (right) Data for paleosol 207TB-9, same as previous. In each paleosol, the largest intensity of the second derivative is from zone 4 of the profile (samples 7D and 9D) and signified by the label I_{535} and dashed black lines. See Figure 2 for profile distribution of zones 1 (A samples), 2 (B samples), 3 (C samples), 4 (D samples), and 5/parent material (E samples).

observed through temperature steps 0–200 °C (Figures 4a–4d), which constrains the Néel temperature of goethite, thus suggesting a lack of this mineral. More of the initial IRM is carried by the low-coercivity (150 mT) component in all cases (Figures 4a–4d). TD patterns demonstrate that the low-coercivity component is not fully demagnetized by the 600 °C heating step, which is higher than the Curie temperature of magnetite at 580 °C. The low-coercivity component persists to the terminal step of 675 °C, practically the Néel temperature of hematite. The high-coercivity (2,500 mT) IRM component also persists to 675 °C. These data suggest the presence of hematite in addition to maghemite and/or oxidized magnetite.

DRS (Figures 2e and 3) and HIRM (Figure 2d) data suggest the presence of hematite within paleosols 207TB-7 and 207TB-9. This hematite must account for at least some if not most of the remanence for the high-coercivity component indicated by the TD results (Figure 4). However, low-temperature oxidation of magnetite at the outcrop may produce a high-coercivity maghemite component (Egli, 2004; van Velzen & Dekkers, 1999). Furthermore, overlapping coercivities of magnetite and maghemite (Geiss et al., 2008) complicate interpreting the contribution of each to the IRM. Another consideration to explain the TD patterns of the IRM is the presence of pigmentous hematite in the paleosols, as suggested by the DRS data. This type of hematite may carry a chemical remanent magnetization that has a range of unblocking temperatures from about 300 to 700 °C (Irving & Opdyke, 1965; Jiang et al., 2015).

TD results in Figures 4b and 4c suggest evidence for a magnetite contribution to the low-coercivity component of sample 207TB-7E (zone 5/parent material) and sample 207TB-9C (zone 3). TD curves for these samples have inflection points at 500 °C (207TB-9C) and 600 °C (207TB-7E) after a nearly linear decrease from the starting temperature of 0 °C. Other samples (Figures 4a and 4d) have a smooth demagnetization curve for the low-coercivity component, from the starting temperature to the terminal TD step of 675 °C.

Back-field IRM data suggest the presence of low-coercivity and high-coercivity magnetic minerals (Figures 5a and 5b). High-coercivity minerals appear to be better represented by the IRM coercivity distribution for the parent material/zone 5 (Figure 5b). The parent material does not fully saturate at the maximum applied field of 2,500 mT and its acquisition pattern has a large curvature. In contrast, zone 3 has a back-field IRM curve that shows saturation by 2,500 mT and a flatter acquisition pattern (Figure 5a). Saturation IRM is only 0.004 Am^2/kg for zone 5/parent material as compared to 0.026 Am^2/kg for zone 3.

4. Discussion

4.1. Vertisol Magnetic Minerals

Magnetic properties and magnetic minerals of ancient Vertisols have not been examined in detail. Three notable Vertisol studies are from the North American subtropics, Buttermilk Creek, USA (Lindquist et al.,

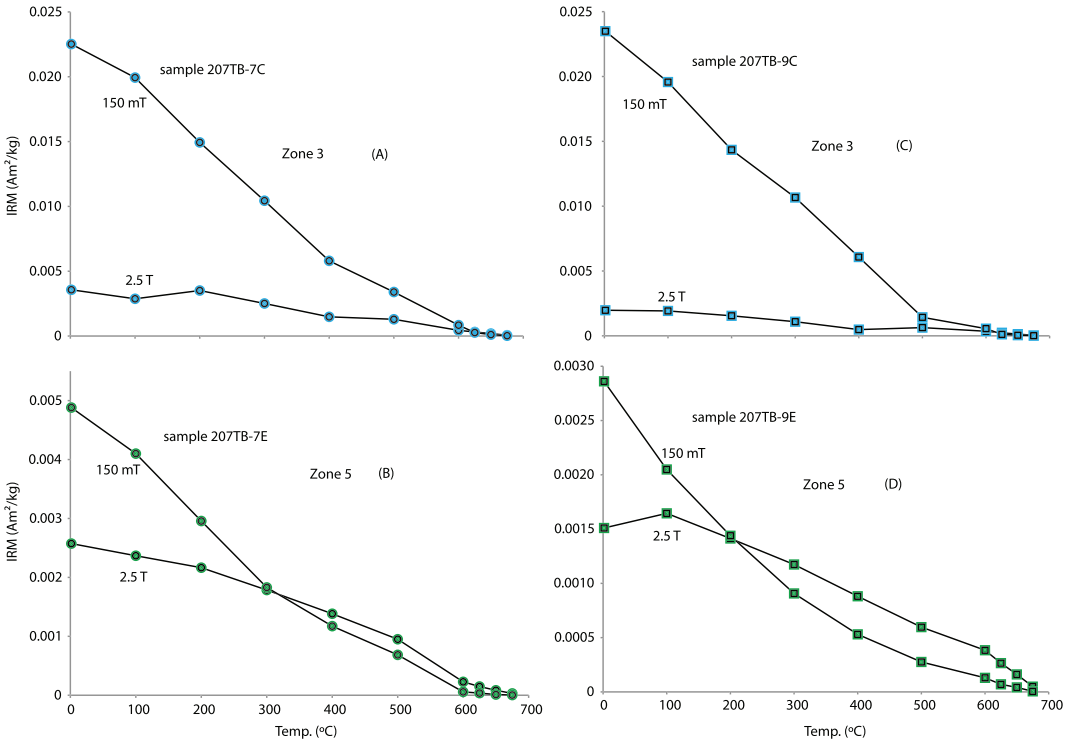

Figure 4. Thermal demagnetization of IRM for parent material (zone 5) compared to zone 3. (a and b) paleosol 207TB-7 and (c and d) paleosol 207TB-9.

2011); the West African tropics, Loulouni, Mali (Fischer et al., 2008); and the European temperate zone, southern Bulgaria (Jordanova & Jordanova, 2016). The Vertisols developed from the latest Pleistocene through to last 1,000 years (USA), during modern times (Mali), and a mixture of Pliocene to recent times (Bulgaria). In all these examples, however, the magnetic minerals are similar. Oxidized magnetite was identified as the main magnetic mineral in the Malian Vertisol (Fischer et al., 2008). In the Vertisol from the USA, magnetite and maghemite were abundant (Lindquist et al., 2011). The main magnetic minerals identified in the three Vertisol profiles from Bulgaria were magnetite, maghemite, and hematite (Jordanova & Jordanova, 2016). DRS and rock magnetic data for the Area 207 paleo-Vertisols suggest a comparable suite of magnetic minerals consisting of hematite and magnetite/maghemite phases.

Area 207 paleo-Vertisols are strongly magnetic. Compared to a worldwide survey based on 272 samples for modern soils (Balsam et al., 2011), only about 10% have mass specific susceptibility values larger than the paleo-Vertisols from Area 207. Maximum mass specific susceptibility values are about 1.5 to 2.5 times larger than the maximum values for the Vertisols from Mali and Texas (Figure 6a). The weakest IRM at 1.0T values for the paleo-Vertisols is 0.004 Am^2/kg (zone 5/parent material of 207TB-9) and 0.006 Am^2/kg (zone 5/parent material of 207TB-7), whereas the strongest values for the Bulgarian Vertisols range at 0.003–0.006 Am^2/kg (Figure 6b). The maximum IRM values for Area 207 varies little whether a magnetic field of 2.5 or 1.0 T field is applied, that is, 0.025 Am^2/kg (1.0 T) and 0.026 Am^2/kg (2.5 T) for zone 3 of 207TB-9.

These strong magnetic intensities for the paleo-Vertisol horizons may result from seasonal redox processes that generate pedogenic ferrimagnetic minerals from ferrihydrite under repeated cycles of anaerobic/aerobic conditions (Jordanova & Jordanova, 2016; Maher, 1998; Taylor et al., 1987). A ferrihydrite precursor may also explain hematite in the Area 207 paleosols. Ferrihydrite typically undergoes dehydration and solid-state rearrangement in the dry monsoon season to form pedogenic hematite (Bigham et al., 2002). Ferrihydrite and goethite are competitive in the same soil environment, with the former having a larger solubility product and favored by a high release rate of Fe ions from parent material (Schwertmann, 1988). TD of orthogonal IRM fields lack indications of goethite in the Area 207 paleosols; although it is meta-stable and may have altered (Berner, 1969).

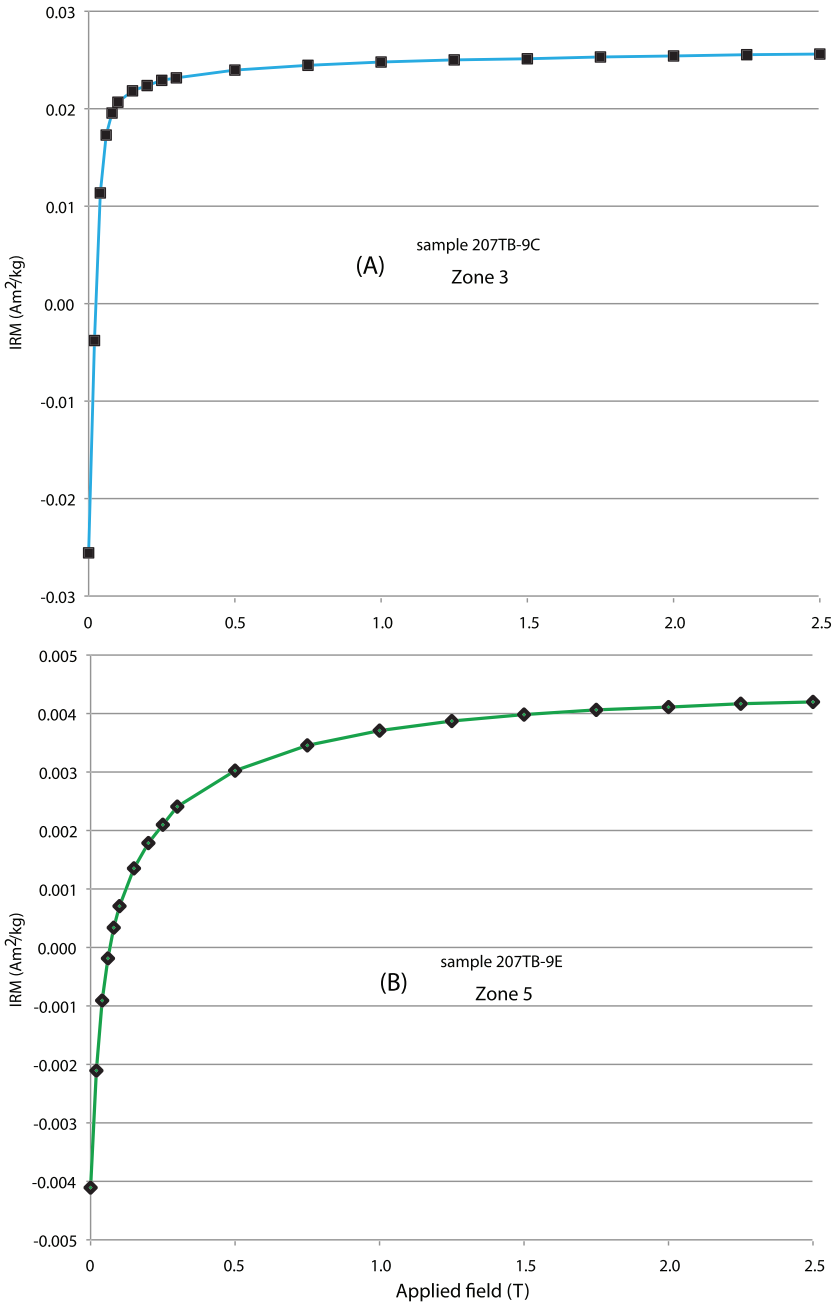

Figure 5. Back-field IRM curves for paleosol for 207TB-9. (a) Zone 3 and (b) zone 5/parent material.

Jordanova and Jordanova (2016) suggest that alluvial Vertisols vary in magnetic intensity due to the concentration of lithogenic magnetic particles in parent material composition. Weathering inputs from igneous parent materials also have strong influences on the resulting soil properties (Ahmad, 1983; Maher, 1998). Basalts may have contributed to the parent material of the Area 207 paleosols as ancient river systems that deposited sediments in the basin flowed near outcroppings of these rocks (Bruhn et al., 2011; Haileab et al., 2004).

Therefore, detrital minerals might be preserved within the Area 207 paleosol samples and biasing the rock magnetic signal. A test of this is a comparison between low-frequency (LF) and high-frequency (HF) susceptibilities (Dearing et al., 1996; Forster et al., 1994). Measured differences between LF and HF (change in susceptibility) values can be plotted against the LF value to obtain an appreciation of the fine-grain

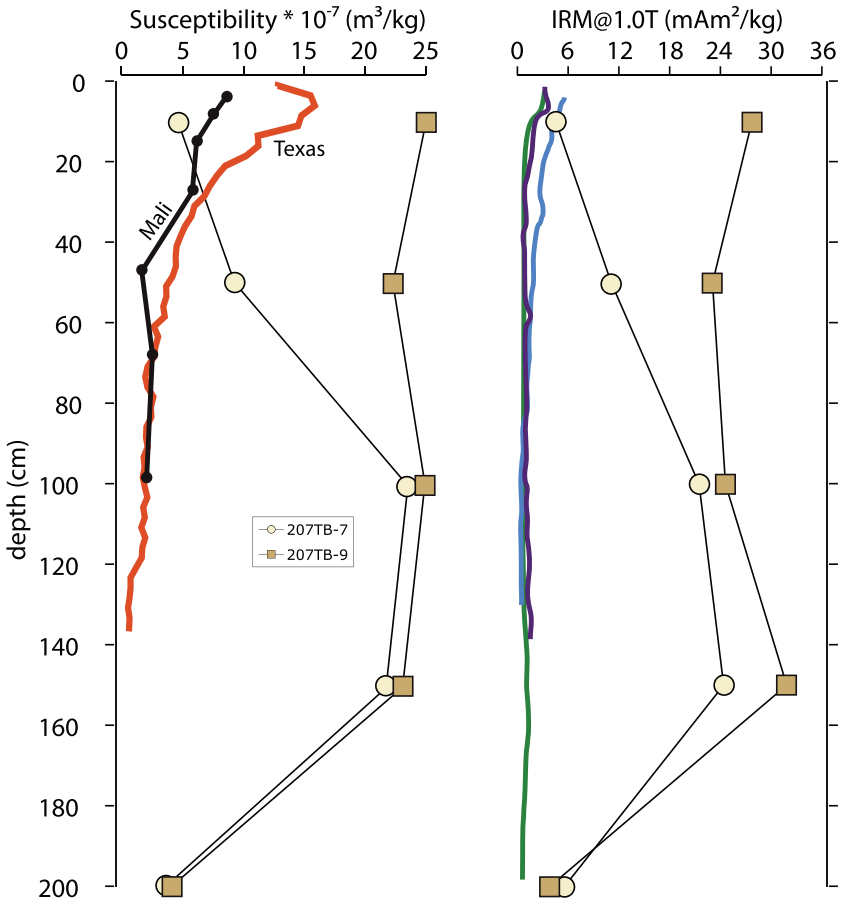

Figure 6. Comparison of magnetic data for seven Vertisols. (a) Mass specific susceptibility of Vertisol from Buttermilk Creek, Texas (Lindquist et al., 2011), Malian Vertisol (Gehring et al., 1997), and paleo-Vertisols 207TB-7 and 207TB-9. (b) IRM at 1.0 T of Bulgarian Vertisols (Jordanova & Jordanova, 2016) compared to paleo-Vertisols 207TB-7 and 207TB-9.

pedogenic fraction of magnetic mineral grains within the samples. Data from the two Area 207 paleosols (Table 1) have almost a perfect linear regression when change in susceptibility is plotted against LF values (individually r^2 = ~0.99 and ~0.93; collectively ~0.99) and the slope of the line is essentially the same for the two sample sets. On such plots, where the line intersects the LF axis is the so-called background susceptibility, which are small and positive values and nearly the same for each paleosol. If the samples solely were comprised of frequency independent magnetic minerals, that is, if the entire sample comprised coarse detrital magnetite, then the HF subtracted from the LF would result in zero. Solving the equation of the linear regression line with a y intercept value of zero by definition results in the x intercept value being equal to the contribution from magnetic minerals with no frequency dependence (Forster et al., 1994). The Area 207 paleo-Vertisols are amenable for this approach because the paleosols were formed on the same parent material and they have strong rock magnetic properties (Dearing et al., 1996). Therefore, to determine the pedogenic fraction of the Area 207 paleosol samples, the background susceptibility is subtracted from the LF values to yield the fine-grained frequency-dependent fraction that is pedogenic in origin (Dearing et al., 1996). The observed linear correlation between the change in susceptibility and the LF values indicate that with increasing magnitude, the bulk susceptibility becomes further controlled by the fine-grained pedogenic

Table 1
Frequency-Dependent Susceptibility Data for Pliocene Vertisols From Area 207[a]

Paleosol	X^B	Level (cm)	X_{LF}	Δ_X	$X^{Pedo.}$
207TB-7	1.6	10	4.3	0.02	2.7
		50	8.5	0.05	6.9
		100	58	0.48	56.4
		150	30.9	0.24	29.3
		200	2.5	0.02	0.9
207TB-9	1.8	10	33.3	0.3	31.5
		50	27.2	0.18	25.4
		100	22.7	0.17	20.9
		150	36.6	0.29	34.8
		200	7.5	0.06	5.7

[a]Expressed as mass dependent susceptibility (10^{-7} m^3 kg^{-1}). See text for discussion.

fraction of magnetic minerals within the samples. Magnetic susceptibility is predicted to increase greatly with decreasing grain size (Maher, 1998). These data distinguish the effects of pedogenic mineral formation from changes in detrital inputs and support the interpretation that the magnetic properties of the Area 207 paleosols are linked to Pliocene pedogenic processes.

4.2. Implications for the Water Table

The position of the water table relative to the developing Vertisol profile influences wetting/drying of the substrate and the closing/opening of cracks and dikes that expose the subsurface to the surface (Wilding & Puentes, 1988). Wetting and closing promotes anaerobic conditions, whereas drying and opening aerates the soil. Water table fluctuations in East Africa are strongly linked with monsoonal seasonality (Nicholson, 2017; Western & Van Praet, 1973).

Zones 1 and 2 of 207TB-7 are the least magnetic of the pedogenically altered horizons for the two paleosols (Figures 2 and 6). However, proxy-indicator values for paleosols 207TB-7 and 207TB-9 become much more similar, if not practically the same at profile depths of zone 3, zone 4, and zone 5/parent material. Low magnetic values may reflect high oxidation, favoring the formation of magnetically weaker hematite (Maher, 1998). DRS/HIRM data do not support this and indicate the uppers zones of 207TB-7 have low hematite (Figures 2d, 2e, and 3).

Water tables perched at shallow depths saturate the soil, creating anaerobic conditions that favor Fe oxide dissolution and inhibit the pedogenesis of ferrimagnets in Vertisols (Jordanova & Jordanova, 2016). Seasonal water commonly ponds at the tops of Vertisols within the gilgai microtopographic lowlands formed between surface mounds (Wilding & Puentes, 1988). The mounds result from the upward displacement of the soil substrate that is necessary to accommodate loose material falling down cracks during the dry season (Ahmad, 1983). Associated with the gilgai microlow of moderately mature to mature Vertisols from the Gulf Coast of Texas, Nordt et al. (2004) documented Fe depletion and high organic carbon in the upper ~50 cm of the profiles. Magnetic minerals overall or ferrimagnetic minerals in particular appear to be in low abundance from the upper ~50 cm of 207TB-7, which is potentially a result of reducing conditions caused by water and organics collected in a gilgai microtopographic low.

Of greater potential significance, however, are the strong magnetic intensities in the lower 100–200 cm of 207TB-7 and the noticeable increase in hematite in zone 4 (Figures 2, 3, and 6). Similar proxy values can be observed in the lower 100–200 cm for 207TB-9. This is notable because it has been hypothesized that Vertisols have shallow water tables, which causes water logging and magnetic dissolution within lower horizons (Fischer et al., 2008; Jordanova & Jordanova, 2016). Consequently, upper Vertisol horizon may appear relatively more magnetic as compared to lower ones because of the reducing conditions in lower horizons. Such processes contribute to the characteristic “magnetic enhancement” of upper Vertisol horizons (Fischer et al., 2008; Jordanova & Jordanova, 2016; Lindquist et al., 2011). Area 207 paleosols obviously differ from these predictions because of the high values for magnetic and DRS data within lower pedogenic horizons (Figures 2, 3, and 6). These data suggest a deep dry season water table, at least deeper than ~150 cm. It also implies that the dry season water table for published examples (Fischer et al., 2008; Jordanova & Jordanova, 2016; Lindquist et al., 2011) was much shallower in comparison, perhaps because their humid/temperate settings afford only limited moisture deficits necessary to retreat the water table to a deeper depth within the profile.

4.3. Paleorainfall During Vertisol Formation in Area 207

One of the more studied issues concerning the Pliocene of East Africa has been the role of paleoclimate contributing to ecosystem change and human evolution (Levin et al., 2011; Quinn & Lepre, 2019; Wynn, 2004). Several hypotheses involve wetter conditions in the Pliocene followed by increased aridity beginning at (~2.6 Ma) the start of the Pleistocene (Cerling et al., 2011; deMenocal, 1995). However, evidence from clumped isotope temperatures of pedogenic carbonates as well as tooth enamel $\delta^{18}O$ values of fossil mammals fail to recognize such a changeover in the Plio-Pleistocene Turkana Basin (Blumenthal et al., 2017; Passey et al., 2010).

Modern East Africa has an overall dry climate that is considered anomalous as compared to other equatorial regions and is likely a consequence of topographic influences of the rift valley and associated volcanic edifices (Nicholson, 2017). Today's Turkana Basin is at a latitude of ~4°N and has two wet monsoonal

seasons during Northern Hemisphere vernal and autumnal months, with summer and winter months experiencing few rainfall events. Mean annual precipitation is approximately 200 mm (average of years 1961 to 1990, NOAA).

The well-represented presence of pedogenic ferrimagnets within the Area 207 paleo-Vertisols (data in Table 1) suggests a well-drained, generally oxidizing soil environment that experienced wet/dry oscillations due to monsoonal seasonality (Ahmed & Maher, 2018). However, zones 3 and 4 of the Area 207 paleosols are the levels at which slickenside development is the greatest as a result of the wetting and drying (Coulombe et al., 1996; Wilding & Puentes, 1988). Effects of monsoonal seasonality on the shrink-swell process are intense at these levels (Ahmad, 1983). Deeper and shallower within the profile, moisture variations contribute less to slickenside development (Yaalon & Kalmar, 1978). Therefore, the best representation of paleoclimate is likely the proxy information associated with zones 3 and 4. Mass specific susceptibility values ($\times m^3/kg$) of zones 3 and 4 fall within the range of 10^{-6} to 10^{-5} (Figure 2). A global study of modern soils, as well as its tropical subset, suggests that pedogenic susceptibility values within this range formed under a mean annual rainfall of about 500–1,000 mm (Balsam et al., 2011). Evidently, this study also determined that pedogenic production of ferrimagnets commences when rainfall exceeds about 200 mm/year. Regional studies of soil magnetic susceptibility (Geiss et al., 2008; Maher et al., 2003) resolve a similar minimal rainfall requirement. In areas that receive greater than about 1,000 mm/year, pedogenic susceptibility decreases (Balsam et al., 2011) probably as a result of reductive dissolution and the flushing of iron from the soil into the groundwater (Sheldon et al., 2002).

An abundance of ferrimagnets, the comparatively low amount of hematite, and the strong intensities for the rock magnetic properties presumably derived from the ferrimagnetic phases all suggest that Pliocene rainfall over Area 207 was greater than today's mean annual rainfall of ~200 mm. Pliocene mean annual rainfall values between 500 and 1,000 mm/year for Area 207 agree with previous estimates for the Turkana Basin. Using depth to paleosol carbonate horizon, Wynn (2004) determined ~700 mm/year at 3.6–3.2 Ma. Ecometric analysis of the fossil mammals by Fortelius et al. (2016) resolved about 500–1,000 mm/year at 4.0–3.0 Ma. At ~3.3 Ma, Blumenthal et al. (2017) interpreted submesic/subxeric conditions from oxygen isotopes of fossil mammal teeth. Whether the present-day aridity of Turkana is something very recent or related to the perceived progressive drying of Plio-Pleistocene East Africa remains to be determined (Polissar et al., 2019).

5. Model of Fe Oxide Production in the Monsoonal paleo-Vertisols of Kenya

Pedogenic models for Vertisols are based upon soils with poor drainage in lower horizons and magnetic enhancement in upper horizons (Fischer et al., 2008; Jordanova & Jordanova, 2016) and therefore are inadequate to explain the modes of production for the interpreted magnetic Fe oxides in the Kenyan paleosols. In fact, most pedogenic models are designed to explain the development of soils that have the greatest magnetic enhancement in upper horizons (Geiss et al., 2008). The Kenyan paleosols appear to be seasonally well drained, similar to soils from Mediterranean areas and the Chinese Loess Plateau (Maher, 2016; Torrent et al., 2010); however, the winter-wet-summer-dry climate is unlike the equinox-wet and solstice-dry monsoon of near-equatorial East Africa.

Large values of mass specific susceptibility for the Kenyan paleosols suggest that a significant fraction of the Fe oxides is represented by ferrimagnets, which are likely magnetite. The wet-dry monsoonal seasonality of East Africa is ideal for the production of soils with high magnetic susceptibilities (Maher, 1998). IRM data also demonstrate magnetite, in addition to hematite to a lesser extent, which is corroborated by the DRS data. Hematite formation is more dependent on temperature and desiccation, but rainfall (moisture) is still needed for hematite precursors to form (Bigham et al., 2002; Schwertmann, 1988).

Abundant hematite and magnetite production in soils results from different environmental parameters. The preservation of magnetite in the Kenyan paleo-Vertisols and the indications of less hematite are explained by the occurrence of an East African monsoon cycle with two wet and two dry seasons. Frequent wetting and drying favors the development of soils with high concentrations of magnetite because the seasonality produces the redox conditions necessary to form the different Fe oxidation states in magnetite (Maher, 2016). Two wet seasons periodically increase ambient soil moisture which emolliates the dryness needed to produce ample concentrations of hematite. Bimodal rainfall seasonality in the equatorial latitudes, due to the

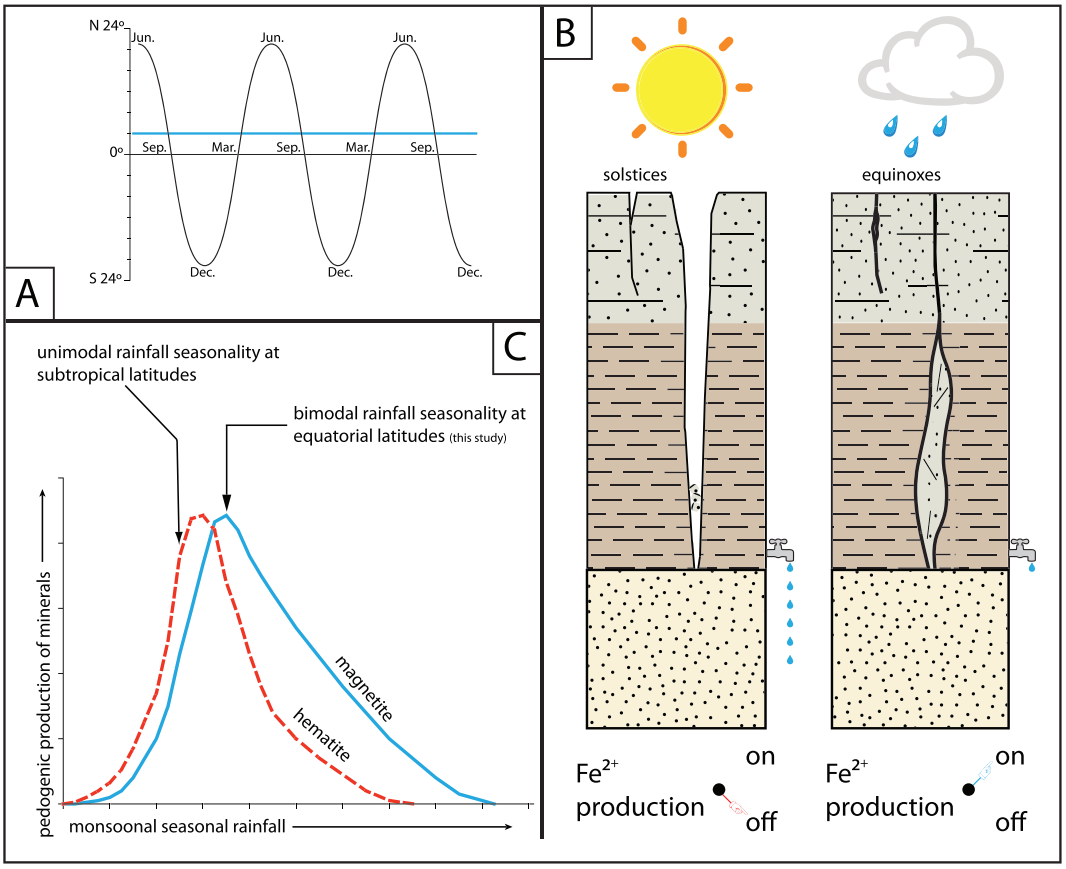

Figure 7. Model of Fe oxide production in the monsoonal paleo-Vertisols of Kenya. (a) Seasonal insolation and rainfall across the tropics. Over the low latitudes, the Sun passes directly overhead twice in a year at the equinoxes, resulting in extreme land-sea temperature contrasts and bimodal rainfall seasonality (Berger & Loutre, 1997; Nicholson, 2017). In contrast, maxiumum insolation reaches the high latitudes once a year at the solstices causing unimodal rainfall seasonality. Blue line is the approximate latitude of the studied paleo-Vertisols in Kenya. (b) Cartoons of Vertisol profiles during dry and wet seasons illustrating morphostructural changes in response to the moisture conditions of the soil substrate. Left profile shows the development of vertical/subvertical cracks under aridity, leading to a well-drained (dripping tap) and aerated oxidating soil environment. Right profile shows a moistened soil environment with expanable clays closing ventilation to the surface. The soil in now poorly drained and anaerobic, ideal for producing ions of reduced iron necessary for magnetite formation. (c) Modified from Balsam et al. (2004). Pedogenic model to explain the occurrence of the magnetic Fe oxides in the paleo-Vertisols from Kenya. Rainfall near subtropical latitudes with only one wet season suffices to generate mostly hematite. More frequent wet/dry oscialltions due to bimodal rainfall seasonality at the low latitudes causes the oxidizing and reducing conditions need to manufacture the Fe^{3+}/Fe^{2+} that form magnetite.

Sun passing directly overhead twice in a year, results in monsoonal wet seasons that recur about every six months at the equinoxes (Berger & Loutre, 1997; Nicholson, 2017; Figure 7a). During the dry seasons at each solstice, the paleo-Vertisols desiccated and the opening of vertical/subvertical cracks at the surface progressively translated downward to the basal horizons of the profile (Figure 7b, left profile). A well-aerated pedogenic substrate via the cracking increased oxidation and generated an environment for Fe^{3+} production. During the equinoxes (Figure 7b, right profile), the paleo-Vertisols were saturated with wet season rainfall. As soil pore spaces filled with water, moistened expandable clays closed cracks that provided ventilation, leading to a rise in Fe^{2+} production under anaerobia. Based on these expectations, subtropical latitudes characterized by one wet monsoon season at a solstice are predicted to develop mostly dry soils with appreciable concentrations of hematite accompanied by relatively low magnetic susceptibility (Figure 7c, red curve). Such soils receive seasonal rains for the hydrolysis of hematite precursors, yet lack significant reduced Fe ions for magnetite production. Increased seasonal contrasts at near-equatorial latitudes as well as a rise in the availability of soil moisture results from a higher mean annual precipitation and the more frequent recurrence of wet seasons. Magnetic susceptibly and other

indicators of Fe oxide composition in these soils reflect an overall increase in ferrimagnets at the expense of hematite (Figure 7c, blue curve).

6. Conclusions

Pliocene alluvial Vertisols that formed in the Turkana Basin of north Kenya have been measured for their Fe oxide composition using rock magnetism and visible light spectroscopy. Downprofile variations of these data lack the erratic changes indicative of multiple unrelated generations of soil formation, suggesting that each paleosol more or less represents a single episode of pedogenesis. These data also lend support to the building consensus that the pedoturbation "inverting" model is inadequate to explain the developmental mechanics for all Vertisols (Driese et al., 2013; Lindquist et al., 2011; Nordt et al., 2004).

The Pliocene Vertisols have strong magnetic intensities derived from the pedogenesis of ferrimagnetic minerals. Proxy indicators demonstrate that ferrimagnetic phases and strong intensities persist down to basal pedogenic horizons of ~100–150 cm, which are also the profile depths that preserve the greatest slickenside development and thus underwent the most intense wetting/drying from monsoonal seasonality. Documented Vertisols from temperate and tropical areas have shallow water tables that cause reductive dissolution of Fe oxides and consequently weak magnetic intensities of these basal horizons. Pliocene Vertisols from Turkana appear to have had a deeper dry season water table in comparison.

Strong bulk rock magnetic intensities and a predominance of ferrimagnets over hematite indicate a Pliocene mean annual rainfall higher than the modern value of ~200 mm/year for Turkana. Magnetic susceptibility values for the strongest pedogenically developed horizons suggest a Pliocene mean annual rainfall between about 500–1,000 mm. This is in agreement with other types of Pliocene environmental evidence from the Turkana Basin.

There is a paucity of research on the Fe oxide composition and rock magnetic properties of Vertisols. Further work is needed to assess whether these Pliocene soils are unique or within the range of natural variations. Especially important is the consideration that soil development throughout East Africa may differ greatly from other near-equator tropical areas because of its bimodal distribution of seasonal rainfall and anomalously dry climate related to the topography of the East African Rift System.

Acknowledgments

AcknowledgementsThe author made all sample collection, measurements, and interpretations alone and therefore takes sole responsibility for any errors. The Kenyan government, Kenyan Wildlife Services, and the National Museums of Kenya are thanked for their permission to conduct research at Lake Turkana and export rock samples to the United States (permit NACOSTI/P/18/31442/23304). The Turkana Basin Institute provided valuable logistical assistance while working at Koobi Fora, Sibiloi National Park, and the town of Ileret. Field and lab work was supported by NSF programs Sedimentary Geology and Paleobiology and Archaeometry (award 1818805). Dennis Kent is thanked for access to the Paleomagnetics Laboratory at Lamont-Doherty and thoughtful discussions about rock magnetism. Three anonymous reviewers offered critiques that greatly improved the quality of this manuscript. The Department of Earth and Planetary Sciences at Rutgers University and department heads are acknowledged for their ongoing support of the Fe-Oxide Lab. Data reported in this study can be accessed through the Open Science Framework at osf.io/j9w2t.

References

Ahmad, N. (1983). Vertisols. In L. P. Wilding, N. E. Smeck, & G. F. Hall (Eds.), *Pedogenesis and Soil Taxonomy. II. The Soil Orders* (pp. 91–123). Amsterdam: Elsevier.

Ahmed, I. A. M., & Maher, B. A. (2018). Identification and paleoclimatic significance of magnetite nanoparticles in soils. *Proceedings of the National Academy of Sciences of the United States of America*, *115*(8), 1736–1741. https://doi.org/10.1073/pnas.1719186115

Balsam, W., Ji, J., & Chen, J. (2004). Climatic interpretation of the Luochuan and Lingtai loess sections, China, based on changing iron oxide mineralogy and magnetic susceptibility. *Earth and Planetary Science Letters*, *223*, 335–348. https://doi.org/10.1016/j.epsl.2004.04.023

Balsam, W., Junfeng, J., Renock, D., Deaton, B. C., & Williams, E. (2014). Determining hematite content from NUV/Vis/NIR spectra: Limits of detection. *American Mineralogist*, *99*, 2280–2291. https://doi.org/10.2138/am-2014-4878

Balsam, W. L., Ellwood, B. B., Ji, J., Williams, E. R., Long, X., & El Hassani, A. (2011). Magnetic susceptibility as a proxy for rainfall: Worldwide data from tropical and temperate climate. *Quaternary Science Reviews*, *30*, 2732–2744. https://doi.org/10.1016/j.quascirev.2011.06.002

Berger, A., & Loutre, M. F. (1997). Intertropical Latitudes and Precessional and Half-Precessional Cycles. *Science*, *278*, 1476–1478. https://doi.org/10.1126/science.278.5342.1476

Berner, R.A., 1969. Goethite stability and the origin of red beds. *Geochimica et Cosmochimica Acta 33*, 267–273. https://doi.org/10.1016/0016-7037(69)90143-4

Beverly, E. J., Lukens, W. E., & Stinchcomb, G. E. (2018). Paleopedology as a Tool for Reconstructing Paleoenvironments and Paleoecology. In D. A. Croft, D. F. Su, & S. W. Simpson (Eds.), *Methods in Paleoecology* (pp. 151–183). Cham: Springer International Publishing. https://doi.org/10.1007/978-3-319-94265-0_9

Bigham, J. M., Fitzpatrick, R. W., & Schulze, D. G. (2002). Iron Oxides. In *Soil Mineralogy with Environmental Applications*, *SSSA Book Series* (pp. 323–366). Madison, WI: Soil Science Society of America. https://doi.org/10.2136/sssabookser7.c10

Bloemendal, J., King, J. W., Hall, F. R., & Doh, S.-J. (1992). Rock magnetism of Late Neogene and Pleistocene deep-sea sediments: Relationship to sediment source, diagenetic processes, and sediment lithology. *Journal of Geophysical Research*, *97*(B4), 4361–4375. https://doi.org/10.1029/91JB03068

Blumenthal, S. A., Levin, N. E., Brown, F. H., Brugal, J.-P., Chritz, K. L., Harris, J. M., et al. (2017). Aridity and hominin environments. *Proceedings of the National Academy of Sciences of the United States of America*, *114*(28), 7331–7336. https://doi.org/10.1073/pnas.1700597114

Brown, F. H., McDougall, I., & Gathogo, P. N. (2013). Age Ranges of Australopithecus Species, Kenya, Ethiopia, and Tanzania. In K. E. Reed, J. G. Fleagle, & R. E. Leakey (Eds.), *The Paleobiology of Australopithecus* (pp. 7–20). Dordrecht, Netherlands: Springer. https://doi.org/10.1007/978-94-007-5919-0_2

Brown, F. H., & Feibel, C. S. (1986). Revision of lithostratigraphic nomenclature in the Koobi Fora region, Kenya. *Journal of the Geological Society*, *143*, 297–310. https://doi.org/10.1144/gsjgs.143.2.0297

Bruhn, R. L., Brown, F. H., Gathogo, P. N., & Haileab, B. (2011). Pliocene volcano-tectonics and paleogeography of the Turkana Basin, Kenya and Ethiopia. *Journal of African Earth Sciences*, *59*, 295–312. https://doi.org/10.1016/j.jafrearsci.2010.12.002

Cande, S. C., & Kent, D. V. (1995). Revised calibration of the geomagnetic polarity timescale for the Late Cretaceous and Cenozoic. *Journal of Geophysical Research*, *100*, 6093–6095. https://doi.org/10.1029/94JB03098

Cerling, T. E. (1984). The stable isotopic composition of modern soil carbonate and its relationship to climate. *Earth and Planetary Science Letters*, *71*, 229–240. https://doi.org/10.1016/0012-821X(84)90089-X

Cerling, T. E., Wynn, J. G., Andanje, S. A., Bird, M. I., Korir, D. K., Levin, N. E., et al. (2011). Woody cover and hominin environments in the past 6 million years. *Nature*, *476*(7358), 51–56. https://doi.org/10.1038/nature10306

Chittamart, N., Suddhiprakarn, A., Kheoruenromne, I., & Gilkes, R. J. (2010). The pedo-geochemistry of Vertisols under tropical savanna climate. *Geoderma*, *159*, 304–316. https://doi.org/10.1016/j.geoderma.2010.08.004

Coulombe, C. E., Wilding, L. P., & Dixon, J. B. (1996). Overview of Vertisols: Characteristics and Impacts on Society. *Advances in Agronomy*, *57*, 289–375.

Dearing, J. A., Dann, R. J. L., Hay, K., Lees, J. A., Loveland, P. J., Maher, B. A., & O'Grady, K. (1996). Frequency-dependent susceptibility measurements of environmental materials. *Geophysical Journal International*, *124*, 228–240. https://doi.org/10.1111/j.1365-246X.1996.tb06366.x

Deaton, B. C., & Balsam, W. L. (1991). Visible Spectroscopy—A Rapid Method for Determining Hematite and Goethite Concentration in Geological Materials. *Journal of Sedimentary Petrology*, *61*, 628–632.

Deckers, J., Spaargaren, O., & Nachtergaele, F. (2001). Vertisols: Genesis, Properties and Soilscape Management for Sustainable Development. In J. K. Syers, F. W. T. Penning de Vries, & P. Nyamudeza (Eds.), *The Sustainable Management of Vertisols* (pp. 3–20). CABI Publishing, New York.

deMenocal, P. D. (1995). Plio-Pleistocene African climate. *Science*, *270*(5233), 53–59. https://doi.org/10.1126/science.270.5233.53

Driese, S. G., Nordt, L. C., Waters, M. R., & Keene, J. L. (2013). Analysis of Site Formation History and Potential Disturbance of Stratigraphic Context in Vertisols at the Debra L. Friedkin Archaeological Site in Central Texas, USA: Analysis of Site Formation History. *Geoarchaeology*, *28*, 221–248. https://doi.org/10.1002/gea.21441

Dudal, R., & Eswaran, H. (1988). Distribution, Properties and Classification of Vertisols. In L. P. Wilding, & R. Puentes (Eds.), *Vertisols: Their Distribution, Properties, Classification and Management* (pp. 1–22). College Station: Texas A&M University.

Egli, R. (2004). Characterization of Individual Rock Magnetic Components by Analysis of Remanence Curves, 1. Unmixing Natural Sediments. *Studia Geophysica et Geodaetica*, *48*, 391–446. https://doi.org/10.1023/B:SGEG.0000020839.45304.6d

Fischer, H., Luster, J., & Gehring, A. U. (2008). Magnetite weathering in a Vertisol with seasonal redox-dynamics. *Geoderma*, *143*, 41–48. https://doi.org/10.1016/j.geoderma.2007.10.004

Forster, T., Evans, M. E., & Heller, F. (1994). The frequency dependence of low field susceptibility in loess sediments. *Geophysical Journal International*, *118*, 636–642.

Fortelius, M., Žliobaitė, I., Kaya, F., Bibi, F., Bobe, R., Leakey, L., et al. (2016). An ecometric analysis of the fossil mammal record of the Turkana Basin. *Philosophical Transactions of the Royal Society B: Biological Sciences*, *371*, 20150232. https://doi.org/10.1098/rstb.2015.0232

Gehring, A. U., Guggenberger, G., Zech, W., & Luster, J. (1997). Combined Magnetic, Spectroscopic, and Analytical-Chemical Approach to Infer Genetic Information for a Vertisol. *Soil Science Society of America Journal*, *61*, 78–85. https://doi.org/10.2136/sssaj1997.03615995006100010013x

Geiss, C. E., Egli, R., & Zanner, C. W. (2008). Direct estimates of pedogenic magnetite as a tool to reconstruct past climates from buried soils. *Journal of Geophysical Research*, *113*, B11102. https://doi.org/10.1029/2008JB005669

Haileab, B., Brown, F. H., McDougall, I., & Gathogo, P. N. (2004). Gombe Group basalts and initiation of Pliocene deposition in the Turkana depression, northern Kenya and southern Ethiopia. *Geological Magazine*, *141*, 41–53. https://doi.org/10.1017/S001675680300815X

Harrison, R. J., & Feinberg, J. M. (2009). Mineral Magnetism: Providing New Insights into Geoscience Processes. *Elements*, *5*, 209–215. https://doi.org/10.2113/gselements.5.4.209

Hillhouse, J. W., Cerling, T. E., & Brown, F. H. (1986). Magnetostratigraphy of the Koobi Fora Formation, Lake Turkana, Kenya. *Journal of Geophysical Research*, *91*, 11581. https://doi.org/10.1029/JB091iB11p11581

Hu, P., Jiang, Z., Liu, Q., Heslop, D., Roberts, A. P., Torrent, J., & Barrón, V. (2016). Estimating the concentration of aluminum-substituted hematite and goethite using diffuse reflectance spectrometry and rock magnetism: Feasibility and limitations: Al-Hematite/Al-Goethite Quantification. *Journal of Geophysical Research: Solid Earth*, *121*, 4180–4194. https://doi.org/10.1002/2015JB012635

Irving, E., & Opdyke, N. D. (1965). The Palaeomagnetism of the Bloomsburg Red Beds and its Possible Application to the Tectonic History of the Appalachians. *Geophysical Journal International*, *9*, 153–167. https://doi.org/10.1111/j.1365-246X.1965.tb02067.x

Jean Pierre, T., Primus, A. T., Simon, B. D., Philemon, Z. Z., Hamadjida, G., Monique, A., et al. (2019). Characteristics, classification and genesis of vertisols under seasonally contrasted climate in the Lake Chad Basin, Central Africa. *Journal of African Earth Sciences*, *150*, 176–193. https://doi.org/10.1016/j.jafrearsci.2018.11.003

Jiang, Z., Liu, Q., Dekkers, M. J., Tauxe, L., Qin, H., Barrón, V., & Torrent, J. (2015). Acquisition of chemical remanent magnetization during experimental ferrihydrite–hematite conversion in Earth-like magnetic field—implications for paleomagnetic studies of red beds. *Earth and Planetary Science Letters*, *428*, 1–10. https://doi.org/10.1016/j.epsl.2015.07.024

Johnson, G. D., & Raynolds, R. G. H. (1976). Late Cenozoic environments of the Koobi Fora formation: the Upper Member along the western Koobi Fora ridge. In Y. Coppens, F. C. Howell, G. L. Isaac, & R. E. Leakey (Eds.), *Earliest Man and Environments in the Lake Rudolf Basin* (pp. 115–123). Chicago: Chicago University Press.

Jordanova, N. (2017). *Soil Magnetism: Applications in Pedology, Environmental Science and Agriculture*. Amsterdam: Elsevier. https://doi.org/10.1016/B978-0-12-809239-2.00005-X

Jordanova, N., & Jordanova, D. (2016). Rock-magnetic and geochemical characteristics of relict Vertisols—signs of past climate and recent pedogenic development. *Geophysical Journal International*, *205*, 1437–1454. https://doi.org/10.1093/gji/ggw067

Kovda, I., Lynn, W., Williams, D., & Chichagova, O. (2001). Radiocarbon Age of Vertisols and Its Interpretation Using Data on Gilgai Complex in the North Caucasus. *Radiocarbon*, *43*, 603–610. https://doi.org/10.1017/S0033822200041254

Kukla, G., Heller, F., Ming, L. X., Chun, X. T., Sheng, L. T., & Sheng, A. Z. (1988). Pleistocene climates in China dated by magnetic susceptibility. *Geology*, *16*, 811–814. https://doi.org/10.1130/0091-7613(1988)016<0811:PCICDB>2.3.CO;2

Leakey, M. G., Feibel, C. S., McDougall, I., Ward, C., & Walker, A. (1998). New specimens and confirmation of an early age for Australopithecus anamensis. *Nature*, *393*(6680), 62–66. https://doi.org/10.1038/29972

Lepre, C. J. (2017). Crevasse-splay and associated depositional environments of the hominin-bearing lower Okote Member, Koobi Fora Formation (Plio-Pleistocene), Kenya. *Depositional Record*, *3*, 161–186. https://doi.org/10.1002/dep2.31

Lepre, C. J., & Kent, D. V. (2015). Chronostratigraphy of KNM-ER 3733 and other Area 104 hominins from Koobi Fora. *Journal of Human Evolution*, *86*, 99–111. https://doi.org/10.1016/j.jhevol.2015.06.010

Levin, N. E., Brown, F. H., Behrensmeyer, A. K., Bobe, R., & Cerling, T. E. (2011). Paleosol carbonates from the Omo Group: Isotopic records of local and regional environmental change in East Africa. *Palaeogeography Palaeoclimatology Palaeoecology*, *307*, 75–89. https://doi.org/10.1016/j.palaeo.2011.04.026

Lindquist, A. K., Feinberg, J. M., & Waters, M. R. (2011). Rock magnetic properties of a soil developed on an alluvial deposit at Buttermilk Creek, Texas, USA. *Geochemistry, Geophysics, Geosystems*, *12*, Q12Z36. https://doi.org/10.1029/2011GC003848

Liu, Q., Roberts, A. P., Torrent, J., Horng, C.-S., & Larrasoaña, J. C. (2007). What do the HIRM and S-ratio really measure in environmental magnetism? *Geochemistry, Geophysics, Geosystems*, *8*, Q09011. https://doi.org/10.1029/2007GC001717

Liu, Q. S., Torrent, J., Barrón, V., Duan, Z. Q., & Bloemendal, J. (2011). Quantification of hematite from the visible diffuse reflectance spectrum: effects of aluminium substitution and grain morphology. *Clay Minerals*, *46*, 137–147. https://doi.org/10.1180/claymin.2011.046.1.137

Long, X., Ji, J., & Balsam, W. L. (2011). Rainfall-dependent transformations of iron oxides in a tropical saprolite transect of Hainan Island, South China: Spectral and magnetic measurements. *Journal of Geophysical Research*, *116*, F03015. https://doi.org/10.1029/2010JF001712

Lowrie, W. (1990). Identification of ferromagnetic minerals in a rock by coercivity and unblocking temperature properties. *Geophysical Research Letters*, *17*, 159–162. https://doi.org/10.1029/GL017i002p00159

Maher, B. A. (1998). Magnetic properties of modern soils and Quaternary loessic paleosols: paleoclimatic implications. *Palaeogeography Palaeoclimatology Palaeoecology*, *137*, 25–54. https://doi.org/10.1016/S0031-0182(97)00103-X

Maher, B. A. (2016). Palaeoclimatic records of the loess/palaeosol sequences of the Chinese Loess Plateau. *Quaternary Science Reviews*, *154*, 23–84. https://doi.org/10.1016/j.quascirev.2016.08.004

Maher, B. A., Alekseev, A., & Alekseeva, T. (2003). Magnetic mineralogy of soils across the Russian Steppe: climatic dependence of pedogenic magnetite formation. *Palaeogeography Palaeoclimatology Palaeoecology*, *201*, 321–341. https://doi.org/10.1016/S0031-0182(03)00618-7

Maher, B. A., & Thompson, R. (1995). Paleorainfall reconstructions from pedogenic magnetic susceptibility variations in the Chinese loess and paleosols. *Quaternary Research*, *44*, 383–391.

McDougall, I., Brown, F. H., Vasconcelos, P. M., Cohen, B. E., Thiede, D. S., & Buchanan, M. J. (2012). New single crystal 40Ar/39Ar ages improve time scale for deposition of the Omo Group, Omo-Turkana Basin, East Africa. *Journal of the Geological Society*, *169*, 213–226. https://doi.org/10.1144/0016-76492010-188

Nicholson, S. E. (2017). Climate and climatic variability of rainfall over eastern Africa: Climate Over Eastern Africa. *Reviews of Geophysics*, *55*, 590–635. https://doi.org/10.1002/2016RG000544

Nordt, L. C., & Driese, S. D. (2010). New weathering index improves paleorainfall estimates from Vertisols. *Geology*, *38*, 407–410. https://doi.org/10.1130/G30689.1

Nordt, L. C., Wilding, L. P., Lynn, W. C., & Crawford, C. C. (2004). Vertisol genesis in a humid climate of the coastal plain of Texas, U.S.A. *Geoderma*, *122*, 83–102. https://doi.org/10.1016/j.geoderma.2004.01.020

Passey, B. H., Levin, N. E., Cerling, T. E., Brown, F. H., & Eiler, J. M. (2010). High-temperature environments of human evolution in East Africa based on bond ordering in paleosol carbonates. *Proceedings of the National Academy of Sciences of the United States of America*, *107*(25), 11,245–11,249. https://doi.org/10.1073/pnas.1001824107

Polissar, P. J., Rose, C., Uno, K. T., Phelps, S. R., & deMenocal, P. (2019). Synchronous rise of African C4 ecosystems 10 million years ago in the absence of aridification. *Nature Geoscience*, *12*(8), 657–660. https://doi.org/10.1038/s41561-019-0399-2

Quinn, R. L., & Lepre, C. J. (2019). Revisiting the pedogenic carbonate isotopes and paleoenvironmental interpretation of Kanapoi. *Journal of Human Evolution*. https://doi.org/10.1016/j.jhevol.2018.11.005

Retallack, G. J. (1988). Field recognition of paleosols. In *Paleosols and Weathering Through Geologic Time: Principles and Applications*, *Geological Society of America Special Papers* (Vol. 216, pp. 1–20). https://doi.org/10.1130/SPE216-p1

Scheinost, A. C., Chavernas, A., Barron, V., & Torrent, J. (1998). Use and Limitations of Second-Derivative Diffuse Reflectance Spectroscopy in the Visible to Near-Infrared Range to Identify and Quantify Fe Oxide Minerals in Soils. *Clays and Clay Minerals*, *46*, 528–536. https://doi.org/10.1346/CCMN.1998.0460506

Schwertmann, U. (1988). Occurrence and Formation of Iron Oxides in Various Pedoenvironments. In J. W. Stucki, B. A. Goodman, & U. Schwertmann (Eds.), *Iron in Soils and Clay Minerals* (pp. 267–308). Dordrecht: Springer Netherlands. https://doi.org/10.1007/978-94-009-4007-9_11

Sheldon, N. D., Retallack, G. J., & Tanaka, S. (2002). Geochemical Climofunctions from North American Soils and Application to Paleosols across the Eocene-Oligocene Boundary in Oregon. *Journal of Geology*, *110*, 687–696. https://doi.org/10.1086/342865

Taylor, R. M., Maher, B. A., & Self, P. G. (1987). Magnetite in soils: I. The synthesis of single-domain and superparamagnetic magnetite. *Clay Minerals*, *22*, 411–422. https://doi.org/10.1180/claymin.1987.022.4.05

Thompson, R., & Oldfield, F. (1986). *Environmental Magnetism*. London Boston Sydney: Allen & Unwin.

Torrent, J., & Barrón, V. (2003). The visible diffuse reflectance spectrum in relation to the color and crystal properties of hematite. *Clays and Clay Minerals*, *51*(3), 309–317. https://doi.org/10.1346/CCMN.2003.0510307

Torrent, J., Liu, Q. S., & Barrón, V. (2010). Magnetic minerals in Calcic Luvisols (Chromic) developed in a warm Mediterranean region of Spain: Origin and paleoenvironmental significance. *Geoderma*, *154*, 465–472. https://doi.org/10.1016/j.geoderma.2008.06.020

Torrent, J., Schwertmann, U., & Schulze, D. G. (1980). Iron oxide mineralogy of some soils of two river terrace sequences in Spain. *Geoderma 23*, 191–208. https://doi.org/10.1016/0016-7061(80)90002-6

van Velzen, A. J., & Dekkers, M. J. (1999). Low-Temperature Oxidation of Magnetite in Loess-Paleosol Sequences: a Correction of Rock Magnetic Parameters. *Studia Geophysica et Geodaetica*, *43*, 357–375.

Western, D., & Van Praet, C. (1973). Cyclical Changes in the Habitat and Climate of an East African Ecosystem. *Nature*, *241*, 104–106. https://doi.org/10.1038/241104a0

Wilding, L. P., & Puentes, R. (1988). *Vertisols: Their Distribution, Properties, Classification, and Management*. College Station: Texas A&M University.

Wu, B., Amelung, W., Xing, Y., Bol, R., & Berns, A. E. (2019). Iron cycling and isotope fractionation in terrestrial ecosystems. *Earth Science Reviews*, *190*, 323–352. https://doi.org/10.1016/j.earscirev.2018.12.012

Wynn, J. G. (2000). Paleosols, stable carbon isotopes, and paleoenvironmental interpretation of Kanapoi, Northern Kenya. *Journal of Human Evolution*, *39*, 411–432. https://doi.org/10.1006/jhev.2000.0431

Wynn, J. G. (2004). Influence of Plio-Pleistocene aridification on human evolution: Evidence from paleosols of the Turkana Basin, Kenya. *American Journal of Physical Anthropology*, *123*(2), 106–118. https://doi.org/10.1002/ajpa.10317

Yaalon, D. H., & Kalmar, D. (1978). Dynamics of cracking and swelling clay soils: Displacement of skeletal grains, optimum depth of slickensides, and rate of intra-pedonic turbation. *Earth Surface Processes*, *3*, 31–42. https://doi.org/10.1002/esp.3290030104